# X-ray-Induced Transformation of *o*-Vinylbenzaldehyde and 2-Methylbenzocyclobutenone to an *o*-Quinoid Ketene and Its Radical Cation

**Krzysztof Huben,[†,‡] Zhendong Zhu,[‡] Thomas Bally,*[,‡] and Jerzy Gebicki*[,§]**

*Contribution from the Institute of Physical Chemistry, University of Fribourg, Pérolles, CH-1700 Fribourg, Switzerland, and Institute of Applied Radiation Chemistry, Technical University of Lodz, 90-924 Lodz, Poland*

*Received December 9, 1996*[⊗]

**Abstract:** Upon ionization in argon matrices by X-irradiation, *o*-vinylbenzaldehyde (**VBA**) partially undergoes transfer of the formyl hydrogen atom to the vinylic $CH_2$ group, thereby forming a quinoketene radical cation of the type previously described (Bally, T.; Michalak, J. *J. Photochem. Photobiol. A: Chem.* **1992**, *69*, 185). This process does not manifest itself clearly in the optical spectra because the transitions of the quinoketene cation coincide with the much more intense ones of **VBA**$^{\bullet+}$ and are mostly obscured by those. However, the IR spectra show unambiguously that the rearrangement occurs rather efficiently. Also they show that in the course of the X-irradiation, the tautomerized cations are reneutralized to from the quinoketene tautomer of **VBA** in good yield. The quinoketene and its radical cation were independently obtained from 2-methylbenzocyclobutenone which undergoes spontaneous ring-opening on photolysis and/or ionization. The optical spectra of the radical cations are assigned on the basis of CASPT2 calculations and the different species involved in this study are characterized at the B3LYP/6-31G* level.

## 1. Introduction

Phototautomerizations (such as for example enolizations of ketones)[1] or photoinduced valence isomerizations (such as pericyclic reactions)[2] represent widely accepted and well-documented phenomena in neutral chemistry. Conversely, the corresponding reactions induced by electron transfer are just beginning to be explored systematically and it is found that they often take a different course than in the neutrals.[3,4] Frequently the order of stabilities of two isomeric forms is reversed by oxidation or reduction such that processes which require activation by light may occur spontaneously in the radical ions. This was found to be the case in several classes of tautomers where enol forms are generally more stable than keto forms. In the case of cycloreversions or ring-opening reactions the order of stabilities is usually not reversed from the neutrals, but the activation barriers are lowered to the extent that the rearrangements occur spontaneously on ionization.[5]

Recently, Kessar et al. found that *o*-vinylbenzaldehyde (**VBA**) undergoes a novel kind of phototautomerization in that it does not form the expected hydroxyvinylallene (**HVA**), but instead reacts from a less stable rotamer to transfer the formyl hydrogen atom and generate an *o*-quinoid ketene, 6-ethylidene-2,4-cyclohexadiene-1-ylidenemethanone (**ECM**). This and the fact that **ECM** could presumably also be generated from 2-methylbenzocyclobuten-1-one (**MBC**)[7,8] led us to investigate the fate of **VBA** and **MBC** on ionization by X-irradiation in solid Ar.

**Scheme 1.** Photochemistry of Neutral *o*-vinylbenzaldehyde (**VBA**)[6]

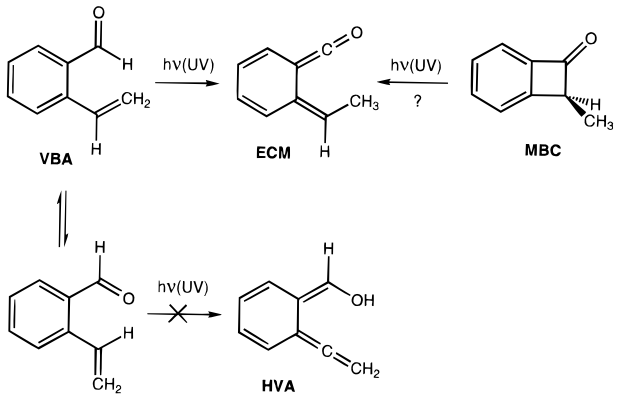


## 2. Methods

**2.1. Syntheses.** *o*-Vinylbenzaldehyde (**VBA**) was prepared from 3,4-dihydroisoquinoline as reported by Dale et al.[9] and purified by distillation (113−115 °C/18 mmHg). 2-Methylbenzocyclobuten-1(2*H*)-one (**MBC**) was obtained by flash vacuum pyrolysis of 2-(1′-hydroxy-1′,2′-dihydro-2′-methylbenzocyclobuten-1′-yl)-2,4-dimethylpentanone,[10] which was in turn prepared by photolysis of 1-(*o*-ethylphenyl)-2,2,4-trimethylpentane-1,3-dione (100 h of irradiation by a 200-W medium-pressure Xe−Hg arc through a Pyrex filter).[10] The precursor

[†] On leave from the Technical University of Lodz, Poland.
[‡] University of Fribourg.
[§] Technical University of Lodz.
[⊗] Abstract published in *Advance ACS Abstracts,* March 1, 1997.

(1) Rappoport, Z., Ed. *The Chemistry of Enols*; Wiley: Chichester, 1990.
(2) See e.g.: Kopecky, J. *Organic Photochemistry: A Visual Approach*; VCH Publishers: New York, 1991; p 77 ff.
(3) (a) Bally, T. In *Radical Ionic Systems*; Lund, A., Shiotani, M., Eds.; Kluwer: Dordrecht, 1991. (b) Gebicki, J. *Pure Appl. Chem.* **1995**, *67*, 55.
(4) Gebicki, J.; Bally, T. *Acc. Chem. Res.* Submitted for publication.
(5) See e.g.: Dunkin, I. R.; Andrews, L. *Tetrahedron* **1985**, *41*, 145. Aebischer, N.; Bally, T.; Roth, K.; Haselbach, E.; Gerson, F.; Qin, X.-Z. *J. Am. Chem. Soc.* **1989**, *111*, 7909.
(6) Kessar, S. V.; Mankotia, A. K. S.; Scaiano, J. C.; Barra, M.; Gebicki, J.; Huben K. *J. Am. Chem. Soc.* **1996**, *118*, 4361.
(7) Hacker, N. P.; Turro, N. J. *J. Photochem.* **1983**, *22*, 131.
(8) Bally, T.; Michalak, J. *J. Photochem. Photobiol. A: Chem.* **1992**, *69*, 185.
(9) Dale, W. J.; Starr, L.; Strobel, C. W. *J. Org. Chem.* **1961**, *26*, 2225.
(10) Yoshioka, M.; Momose, S.; Nishizawa, K.; Hesagawa, T. *J. Chem. Soc., Perkin Trans. 1* **1992**, 499. The pyrolysis in the inlet of the GC column did not work in our experience.

S0002-7863(96)04243-6 CCC: $14.00 

dione was obtained by condensation of 2,4-dimethylpentan-3-one with *o*-ethylbenzaldehyde followed by Jones oxidation.[11]

**2.2. Matrix Isolation and Spectroscopy.** A 1:1 mixture of **VBA** or **MBC** and $CH_2Cl_2$ (which acts as an electron scavenger) was diluted with a 1000-fold excess of argon and deposited on a CsI plate held at 20 K. After the sample was cooled to the lowest temperature attainable by the closed-cycle cryostat (12 K), the sample was exposed to 90 min of X-irradiation as described previously.[3,12] Photolyses were effected with a 1 kW Ar plasma arc with use of interference filters.

Electronic absorption (EA) spectra were taken between 190 and 1500 nm with a Perkin Elmer Lambda 19 instrument whereas IR spectra were obtained on a Bomem DA3 interferometer (1 $cm^{-1}$ resolution) equipped with an MCT detector (500−4000 $cm^{-1}$).

**2.3. Quantum Chemical Calculations.** The geometries of all species were optimized by the B3LYP density functional method[13] as implemented in the Gaussian 94 suite of programs,[14,15] using the 6-31G* basis set. All potential energy minima for the most stable rotamers (and, in the case of neutral **VBA**, also those of the others) were identified by Hessian calculations which yielded also some valuable information on the IR spectra.

Excited state calculations on the radical cations were carried out at the B3LYP/6-31G* geometries by the CASSCF/CASPT2 procedure[16] with the MOLCAS program.[17] The $\pi$ excited states were calculated with a ($9\pi$,$10\pi$) active space.[18] In order to ensure orthogonality, the CASSCF wave function was averaged over the five lowest $\pi$ excited states which resulted in a satisfactory description of these. In all cases the final CASPT2 states were described to >65% by the first-order CASSCF wave function and no single state outside the active space contributed by more than 1%. Any attempt to calculate higher excited states resulted in severe problems with intruder states in the CASPT2 part whose remediation would have required an extension of the active space beyond the limits imposed by the program and hardware. Due to the expected small oscillator strengths of $\sigma \rightarrow \pi$ transitions, $\sigma$ states were not considered. Satisfactory agreement with experiment was obtained with the simple [C]3s2p1d/[H]2s ANO DZ basis set,[19] therefore we saw no necessity to add higher angular momentum and/or diffuse functions. Transition moments were calculated on the basis of the CASSCF wave functions, using CASPT2 energy differences in the denominator.

## 3. Results

Our experimental findings are summarized in Figure 1 (electronic absorption, EA) and Figure 2 (IR spectra). There, traces

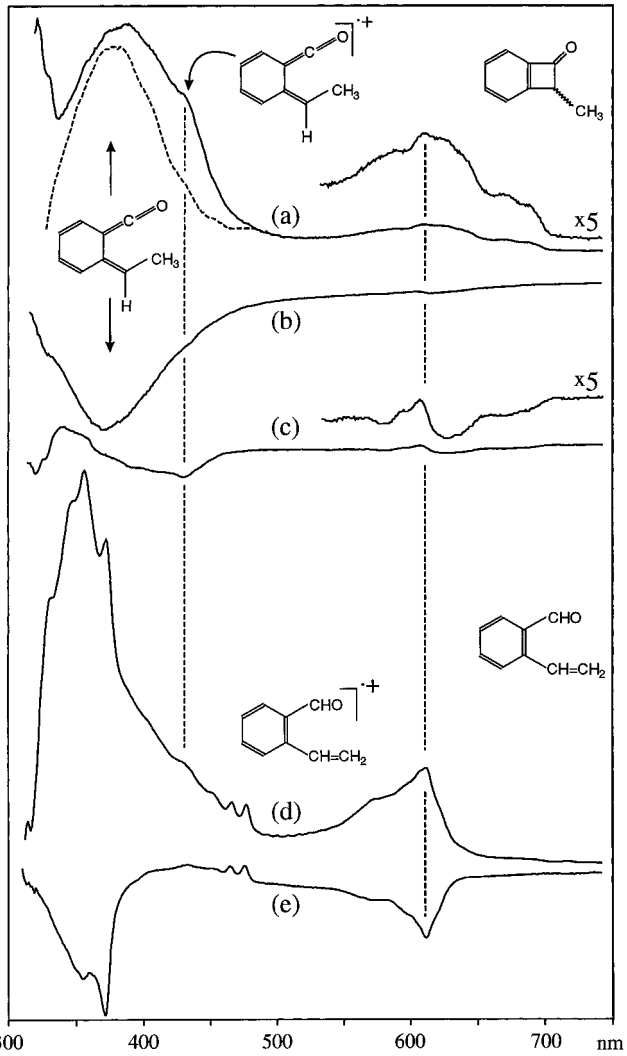


**Figure 1.** (a) Difference spectrum after 90 min of X-irradiation of **MBC** (the dashed line is the difference spectrum for 15 min of photolysis of **MBC** or **VBA** through a Pyrex filter); (b) difference spectrum for photolysis of the above sample at 365 nm and (c) for subsequent 6 h of photolysis at >420 nm; (d) difference spectrum after 90 min of X-irradiation of **VBA** and (e) after subsequent 45 min of photolysis at 600 nm.

(a) show the spectral changes on X-irradiation of **MBC** while the dashed lines indicate the changes on UV photolysis of **MBC**. In both experiments **MBC** with its intense pair of IR peaks at 1776 and 1811 $cm^{-1}$ undergoes ring-opening to the *o*-quinoid ketene, **ECM**,[8] which distinguishes itself by the characteristic group of peaks near 2100 $cm^{-1}$ (strongly split by site effects) and by a broad EA band with $\lambda_{max}$ = 380 nm (dashed lines).[7,8] In addition to these features, X-irradiation gives rise to new IR peaks around 2170 $cm^{-1}$ and indicates also the loss of some CO (2143 $cm^{-1}$), whereas the EA spectrum shows a shoulder at 430 nm and a weak, broad band peaking at 610 nm.

Subsequent photolysis of the X-irradiated sample at 365 nm leads to the disappearance of the 380-nm band and the associated ketene stretching bands in the IR while the 1776/1811-$cm^{-1}$ peaks of **MBC** reappear concomitantly, thus confirming the photoreversibility of the (neutral) ring-opening reaction. In addition, a new IR peak grows in at 1706 $cm^{-1}$, which is due to one of the rotamers of *o*-vinylbenzaldehyde (**VBA**),[6] as will be shown below (note that the same peak had already appeared weakly after X-irradiation of **MBC**). Conversely, the IR bands at 2170 $cm^{-1}$ as well as the EA bands at 420 and 610 nm remain virtually unaffected by this photolysis. Only on prolonged

(11) Nielsen, A. T.; Gibbons, C.; Zimmerman, C. A. *J. Am. Chem. Soc.* **1951**, *73*, 4696.

(12) Bally, T. *Chimia* **1994**, *48*, 378.

(13) (a) Becke, A. D. *Phys. Rev. A* **1988**, *39*, 3098. (b) Becke, A. D. *J. Chem. Phys.* **1993**, *98*, 5648. (c) Lee, C.; Yang, W.; Parr, R. G. *Phys. Rev. B* **1988**, *37*, 785.

(14) Frisch, M. J.; Trucks, G. W.; Schlegel, H. B.; Gill, P. M. W.; Johnson, B. G.; Robb, M. A.; Cheeseman, J. R.; Keith, T.; Petersson, G. A.; Montgomery, J. A.; Raghavachari, K.; Al-Laham, M. A.; Zakrzewski, V. G.; Ortiz, J. V.; Foresman, J. B.; Cioslowski, J.; Stefanov, B. B.; Nanayakkara, A.; Challacombe, M.; Peng, C. Y.; Ayala, P. Y.; Chen, W.; Wong, M. W.; Andres, J. L.; Replogle, E. S.; Gomperts, R.; Martin, R. L.; Fox, D. J.; Binkley, J. S.; DeFrees, D. J.; Baker, J.; Stewart, J. P.; Head-Gordon, M.; Gonzalez, M.; C.; Pople, J. A. *Gaussian, Inc.*; Pittsburgh: PA, 1995.

(15) For a description of the density functionals as implemented in the Gaussian series of programs, see: Johnson, B. G.; Gill, P. M. W. L.; Pople, J. A. *J. Chem. Phys.* **1993**, *98*. 5612.

(16) (a) Andersson, K.; Malmqvist, P.-Å.; Roos, B. O.; Sadlej A. J.; Wolinski, K. *J. Phys. Chem.* **1990**, *94*, 5483. (b) Andersson, K.; Malmqvist, P.-Å.; Roos, B. O. *J. Chem. Phys.* **1992**, 96, 1218. (c) Andersson, K.; Roos, B. O. In *Modern Electronic Structure Theory*; World Scientific Publishing: Singapore, 1995; Part 1, Vol. 2, p 55.

(17) Molcas, Version 3: Andersson, K.; Blomberg, M. R. A.; Fülscher, M. P.; Kellö, V.; Lindh, R.; Malmqvist, P.-Å.; Noga, J.; Olsen, J.; Roos, B. O.; Sadlej, A.; Siegbahn, P. E. M.; Urban M.; Widmark, P.-O. University of Lund: Sweden, 1994.

(18) In the case of $\mathbf{VBA}^{\bullet+}$ we found it necessary to include the next higher virtual $\pi$-MO to arrive at a satisfactory description of all $\pi$ excited states of interest, resulting in a (9,11) active space.

(19) Widmark, P.-O.; Malmqvist, P.-Å.; Roos, B. O. *Theor. Chim. Acta* **1990**, *77*, 291.

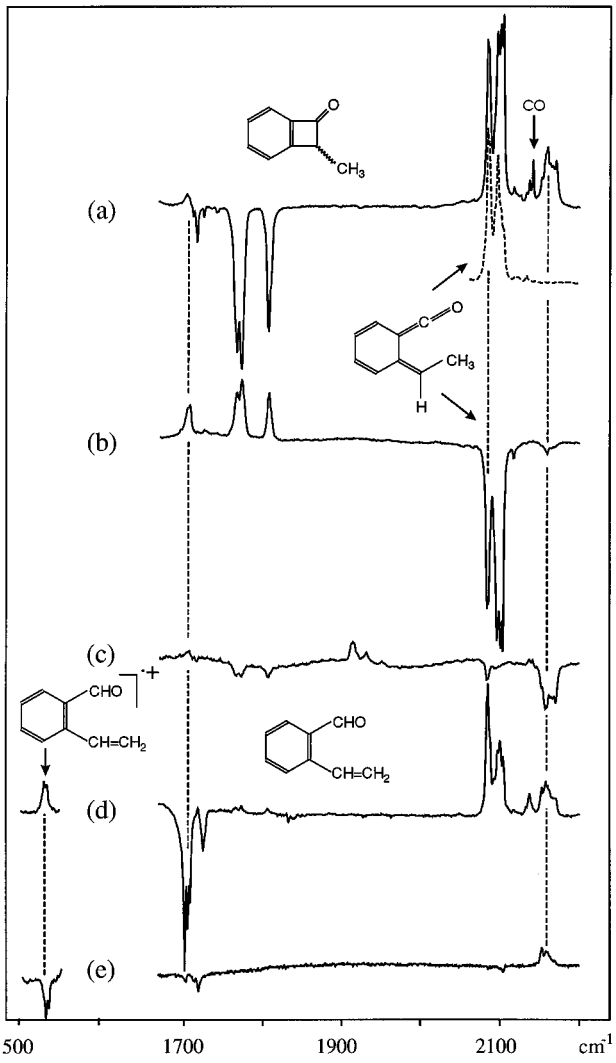


**Figure 2.** IR spectra for steps (a)−(e) as described in the caption to Figure 1.

irradiation at >420 nm do we note a slight decrease in these features, as illustrated in traces (c).

Building on the recent results of Kessar et al., who found that **ECM** is also formed from **VBA** on photolysis,[6] and on our own earlier work on ionization-induced tautomerizations,[4] we endeavored to investigate the fate of **VBA** on ionization. The corresponding results are shown in the last two traces of Figures 1 and 2. Spectra (d) show that X-irradiation of **VBA** (see strong IR peaks around 1710 $cm^{-1}$) leads also to formation of **ECM** as well as the other group of IR bands around 2170 $cm^{-1}$. In the UV/vis range we note the appearance of a strong pair of peaks at 355/370 nm in addition to a weaker band at 610 nm and some wiggles around 470 nm.

In contrast to the above experiments starting from **MBC**, bleaching of the visible EA bands was quite efficient in this case: 45 min of irradiation through a 600 nm interference filter sufficed to remove the blue band and the 355/370 nm pair of peaks (trace (d)) which left essentially the broad **ECM** band at 380 nm and the wiggles around 470 nm. The latter proved to be photostable whereas neutral **ECM** showed the same bleaching behavior as illustrated in spectra (b) above. In searching for features in the IR spectrum which rise and fall in concert with the new optical absorptions detected after X-irradiation, we only found a relatively weak peak at 1534 $cm^{-1}$ which decays on bleaching while the group of IR peaks at 2170 $cm^{-1}$ rises.

## 4. Discussion

**4.1. Mechanistic Aspects.** There is a considerable body of experience which shows that X-irradiation of organic molecules M embedded in argon matrices together with some electron scavenger S ($CH_2Cl_2$ in our case) leads primarily to formation of the corresponding radical cations $M^{\bullet+}$ through hole transfer from ionized argon while the electrons are trapped by forming $S^{\bullet+}$.[3a,12] In addition we found recently that, once formed, the radical cations appear to compete efficiently with S for the electrons which are liberated in the process of X-irradiation and are thus reneutralized.[8] This process limits the yield of charged species that can be obtained in such experiments, but it usually goes unnoticed because it re-forms the starting M. However, if $M^{\bullet+}$ *spontaneously* undergoes some rearrangement to isomeric $N^{\bullet+}$ (or loses a fragment such as molecular nitrogen), then re-neutralization leads to formation of neutral N which may be a photoproduct of M (cf. Scheme 2). In principle, this mechanism allows the net M → N rearrangement to be carried to completion which is not always possible otherwise.[4]

**Scheme 2.** Mechanism for the Formation of Neutral Rearranged Products **N** by Way of Ionization/ Reneutralization on X-irradiation of Argon Matrices

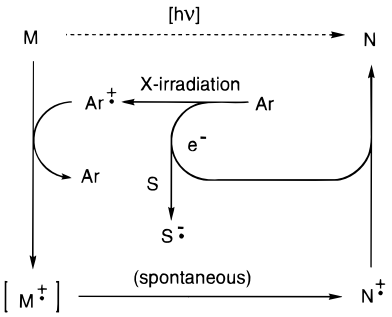


We believe that all of the events observed in the present work and described above can be explained on the basis of these three processes, i.e. *ionization*, *rearrangement*, and *re-neutralization*. Thus, upon ionization in argon, both **MBC** and **VBA** appear to undergo spontaneous rearrangement to $\mathbf{ECM}^{\bullet+}$, the former by ring-opening, the latter by transfer of the formyl hydrogen atom. Whereas the rearrangement appears to be complete in the case of **MBC** (as in the parent molecule,[8] we could find no trace of $\mathbf{MBC}^{\bullet+}$), it is only partial in $\mathbf{VBA}^{\bullet+}$, which manifests itself clearly in the EA spectrum (see below) and less obviously but still distinctly in the IR (1534-$cm^{-1}$ peak). In both cases we find substantial quantities of neutral **ECM** which is presumably formed by re-neutralization of its radical cation. On X-irradiation of **MBC** we also notice some neutral **VBA** (IR band

**Scheme 3.** Formation of **ECM** and Its Radical Cation from **VBA** or **MBC**

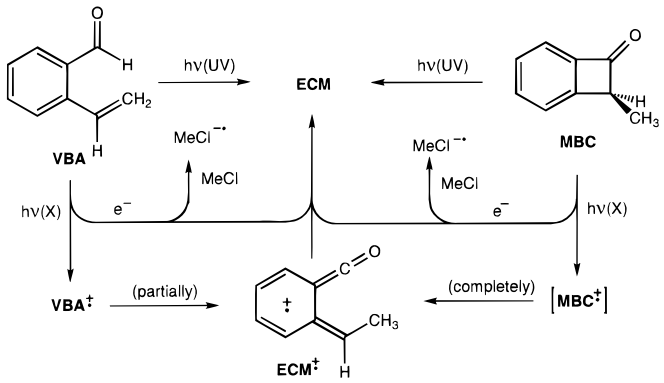

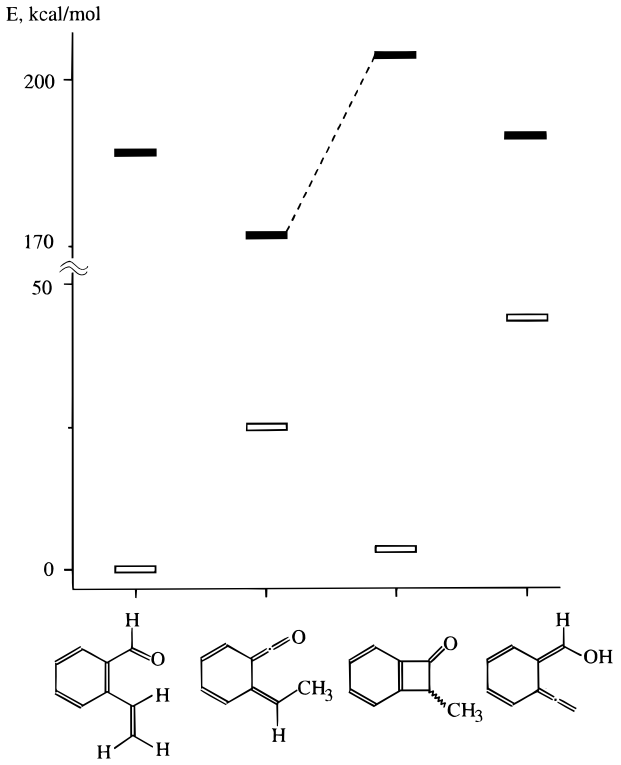


**Figure 3.** Schematic representation of the energies of four neutral (open bars) and cationic (solid bars) $C_9H_8O$ isomers relative to neutral **VBA** as obtained by B3LYP/6-31G* calculations. Only the energies of the most stable rotamers (drawn at the bottom) are plotted; those of the less stable rotamers are listed in Table 1. All energies are at equilibrium geometries except that for **MBC**$^{\bullet+}$ (which collapses spontaneusly to **ECM**$^{\bullet+}$), which is given at the neutral equilibrium geometry.

at 1706 cm$^{-1}$) which may arise by way of ionization and subsequent rearrangement and reneutralization from the secondary product, **ECM**. However, the virtual absence of the strong EA bands of **VBA**$^{\bullet+}$ in these experiments would seem to suggest that **VBA** may also be formed by another mechanism in this case.

**4.2. Energetics and Vibrational Structure.** In order to substantiate our propositions and assignments, and to gain more detailed insight into the behavior of different **VBA** conformers, we carried out quantum chemical calculations. Table 1 and Figure 3 show the results of the B3LYP/6-31G* calculations on **VBA, ECM, MBC**, and their radical cations, including also the other possible product of H-transfer from **VBA**, i.e. the *o*-quinoid hydroxyvinylallene, **HVA**. Analogous to earlier cases of spontaneous hydrogen transfer reactions of radical cations,[4] we note the marked changes in relative stabilities of **VBA** and the two H-shifted products on ionization. The same applies to the pair of valence isomers, **MBC** and **ECM**.

Firstly, we would like to comment on the different conformers of neutral **VBA** from which ionization may occur. B3LYP/6-31G*, which gives rotational barriers for styrene and benzaldehyde in good agreement with experiment,[20] predicts the most stable of these to be the *s,a*-conformer followed by the *a,a*-conformer. This order of stabilities may appear surprising at first sight, but we think that it can be explained on the basis of the geometric features of the formyl group (cf. Scheme 4).

Due to the small exocyclic C−C−H angles in benzaldehyde and styrene the two hydrogens come in very close contact in the planar *a,a*-conformer, thus necessitating a significant twisting of the vinyl group (and to a smaller degree even of the formyl group) to avoid steric strain. Conversely, the large C−C═O angle (which is even widened by 3° in *s,a*-**VBA**) allows for more planarity in the *s,a*-conformer which may furthermore profit from a weak stablizing interaction between the vinylic hydrogen and the carbonyl oxygen.

The "reactive" *a,s*-conformer is even higher in energy than the former two, whereas the *s,s*-conformer need not be considered in the calculation of the equilibrium composition. After transformation of the energy differences into $\Delta G_{298K}$ (based on the B3LYP structures and vibrations), these translate into an equilibrium composition of the *s,a*-, *a,a*-, and *a,s*-conformers of 78.8%:15.8%:5.4%. Hence most of the neutral **VBA** is predisposed for formation of *s*-**HVA** whereas only a

(20) (a) Styrene: calculated 4.42 kcal/mol, experimental 4 ± 0.4 kcal/mol (Facchine, K. L.; Staley, S. W.; van Zijl, P. C. M.; Mishra, P. K.; Bother-By, A. A. *J. Am. Chem. Soc.* **1988**, *110*, 4900. (b) Benzaldehyde: calculated 9.92 kcal/mol, experimental (NMR, $\Delta H^{\ddagger}$) 8.3 ± 0.2 kcal/mol (Lunazzi, L.; Macciantelli, D.; Baicelli, A. C. *Tetrahedron Lett.* **1975**, 1205). Note that there is a discrepancy between the rotational barrier of benzaldehyde from NMR and from IR measurements, the latter giving much lower values which are, however, in disaccord with all calculations (cf.: Head-Gordon, M.; Pople, J. A. *J. Phys. Chem.* **1993**, *97*, 1147).

**Table 1.** Energies of Different $C_9H_8O$ Isomers and Their Radical Cations from B3LYP/6-31G* Calculations[a]

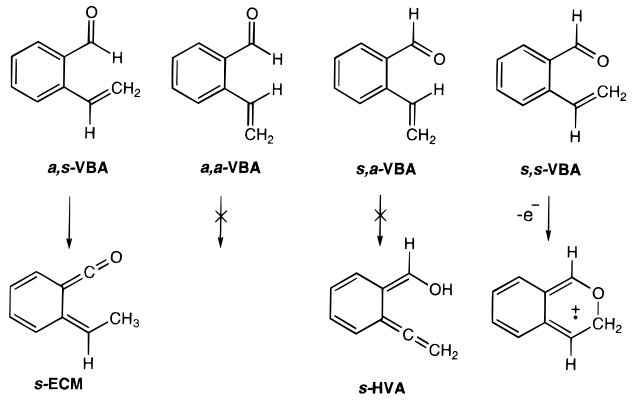


| | neutral | radical cation |
|---|---|---|
| *s,a*-**VBA** | −422.96906[b] | −422.67018[b] |
| *a,a*-**VBA** | +0.81 [+0.95][c] | +3.97 |
| *a,s*-**VBA** | +1.54 [+1.58][c] | +4.85 |
| *s,s*-**VBA** | +3.74 | (−22.16)[d] |
| **MBC** | +3.86 | +16.61[e] |
| *s*-**ECM** | +24.11 | −13.86 |
| *s*-**HVA** | +43.94 | +6.14 |

[a] Except where noted all energies are in kcal/mol relative to *s,a*-**VBA** or its radical cation and correspond to fully optimized structures that are available in the Supporting Information. [b] Total energies in hartrees. [c] Difference in $\Delta G$(298K). [d] *s,s*-**VBA** collapses to an *o*-quinoid pyran on ionization (cf. scheme above). [e] At the geometry of netural **MCB** (cation collapses to **ECM**$^{\bullet+}$ on optimization).

**Scheme 4.** B3LYP/6-31G* Geometries of *s,s*- and *a,s*-**VBA** compared to those of benzaldehyde and styrene

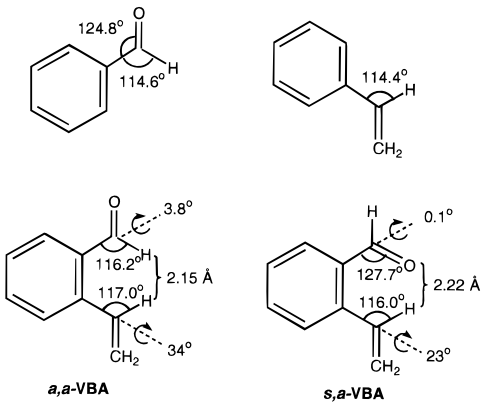

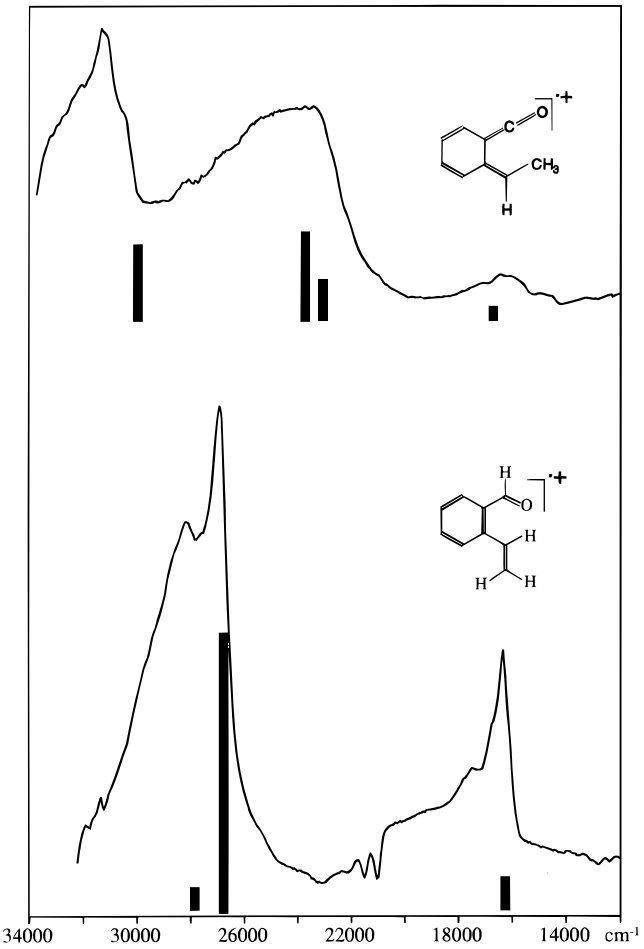


**Figure 4.** EA spectra of **VBA**$^{\bullet+}$ (= difference spectrum (e) in Figure 1 reversed) and **ECM**$^{\bullet+}$ (= spectrum (a) in Figure 1 minus that of neutral **ECM**) on a wavenumber scale and CASPT2 predictions (cf. Tables 2 and 3).

small percentage can directly yield *s*-**ECM** (or the respective cations after ionization).

However, B3LYP/6-31G* predicts that the **VBA** → **HVA** rearrangement is strongly endothermic, which is perhaps the reason why no allenic or OH stretching vibrations were observed after photolysis of **VBA**.[21] Although strongly attenuated, the endothermicity of this process persists in the radical cation which may explain why we found no sign of **HVA**$^{\bullet+}$ after ionization of **VBA**,[22] in contrast to the exothermic rearrangement to **ECM**$^{\bullet+}$. If the rearrangement to **HVA**$^{\bullet+}$ does not occur, then most of the **VBA** will retain its structure after ionization, i.e. the yield of **VBA**$^{\bullet+}$ is expected to be much larger than that of **ECM**$^{\bullet+}$ in those experiments. Nevertheless, the latter may show up more prominently in the IR spectra due to the exceptionally high intensity of the ketene stretching vibration. Neutral **ECM** appears most strongly because it continues to be formed (by re-neutralization of **ECM**$^{\bullet+}$, cf. Scheme 2) in the course of X-irradiation.

(21) The energy of the photons used in the **VBA** photolysis[6] would have sufficed to make up for the endothermicity, but perhaps the "funnels" on the excited state surface are ill disposed for relaxation to **HVA**. Also, our calculations show that the vinylic proton remains coordinated to the incipient allenic $\pi$-bond after its transfer to the carbonyl group (i.e. formation of **HVA**). This may cause the barrier for re-ketonization to be too small for **HVA** to persist after photolytic formation. A calculation of the corresponding reaction path could elucidate this possibility.

(22) We believe that the small IR bands which rise around 1900 cm$^{-1}$ on exhaustive photolysis of **MBC**$^{\bullet+}$ are *not* due to HVA$^{\bullet+}$ because this would necessitate previous formation of **VBA**$^{\bullet+}$, which is not observed in this experiment. They are probably due to an allenic product of ring-opening that may be formed in a single step.

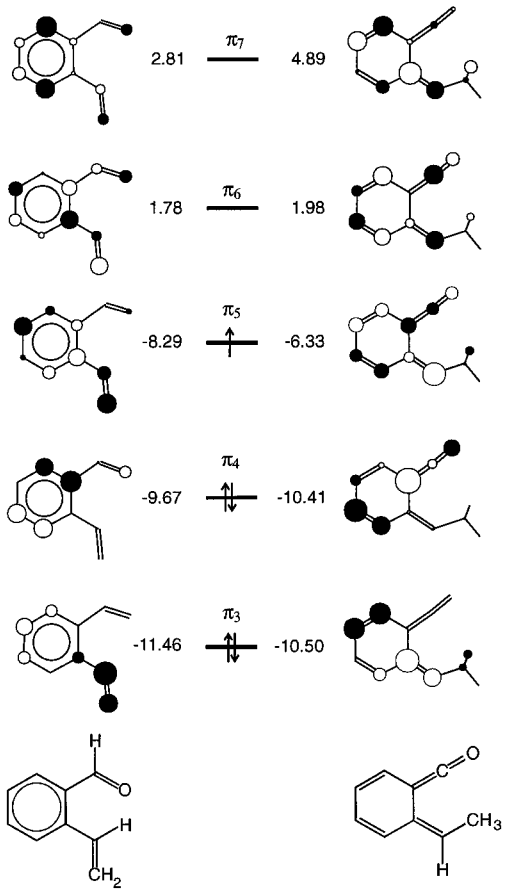


**Figure 5.** MOs of **VBA** and **ECM** involved in the electronic transitions of their radical cations listed in Tables 2 and 3.

In contrast to parent benzocyclobutenone,[8] we found the ring-opening of **MBC**$^{\bullet+}$ to be entirely activationless. This is presumably due to the stabilization of the lowest $\sigma$ state (which is dissociative with regard to ring-opening)[8] by the inductive effect of the methyl group, so that it falls below the $\pi$ ground state of the parent cation. Hence, vertical ionization of **MBC** leads directly to a dissociative surface. But even if a $\pi$ state would be attained vertically, breaking of the $C_s$ symmetry by the methyl group entails a mixing of $\pi$ and $\sigma$ states, which may lead to the disappearance of the symmetry-imposed barrier for the ring-opening of the parent cation.[8] In fact, no potential energy minimum could be located for **MBC**$^{\bullet+}$ (the black bar in Figure 3 indicates the cation's energy at the neutral geometry). Finally we note that we could not find a local minimum corresponding to the ionized form of the least stable **VBA** rotamer (*s*,*s*) which undergoes spontaneous ring closure to a much more stable quinoid pyran cation (cf. Table 1).

The calculated IR spectra of the different cations show also features which are in general agreement with our observations: on ionization of **ECM**, the calculated ketene stretching frequency *increases* by 58 cm$^{-1}$ (experimentally 50−70 cm$^{-1}$) because the HOMO of **ECM** is slightly C═O antibonding (cf. Figure 5). Conversely, the C═O stretching frequency of **VBA** is predicted to decrease by a similar amount which puts it unfortunately in the region where water molecules associated with the very polar **VBA** show strong, sharp peaks (not shown in Figure 2). However, the most intense IR band of **VBA**$^{\bullet+}$ is predicted at 1583 cm$^{-1}$, in good accord with our observation of the only band which we attribute to this cation at 1534 cm$^{-1}$.

**4.3. Electronic Structure of Radical Cations.** To gain some insight into the electronic structure of the radical cations whose EA spectra we have observed in this study we embarked

**Table 2.** Excited States of **VBA**$^{\bullet+}$ [a] by CASSCF/CASPT2

| | CASSCF[b] | | CASPT2 | | | |
|---|---|---|---|---|---|---|
| state | $E_{rel}$/eV | composition[c] | $E_{rel}$/eV | $f$[d] | % ref[e] | exp $E_{rel}$/eV[f] |
| $1^2A''$ [g] | (0) | 80% ... $(\pi_3)^2(\pi_4)^2(\pi_5)^1$ | (0) | | 71 | (0) |
| $2^2A''$ | 1.25 | 76% ... $(\pi_3)^2(\pi_4)^1(\pi_5)^2$ | 1.16 | 0.001 | 71 | |
| $3^2A''$ | 2.26 | 54% ... $(\pi_3)^1(\pi_4)^2(\pi_5)^2$ | 2.00 | 0.040 | 70 | 2.03 |
| | | 19% ... $(\pi_3)^2(\pi_4)^2(\pi_5)^0(\pi_6)^1$ | | | | |
| $4^2A''$ | 3.76 | 45% ... $(\pi_2)^1(\pi_3)^2(\pi_4)^2(\pi_5)^2$ | 3.46 | 0.031 | 69 | ($\approx$3.5) |
| | | 17% ... $(\pi_3)^2(\pi_4)^2(\pi_5)^0(\pi_7)^1$ | | | | |
| $5^2A''$ | 4.31 | 45% ... $(\pi_3)^2(\pi_4)^2(\pi_5)^0(\pi_6)^1$ | 3.30 | 0.431 | 64 | 3.33 |
| | | 18% ... $(\pi_3)^1(\pi_4)^2(\pi_5)^2$ | | | | |
| | | 5% ... $(\pi_2)^1(\pi_3)^2(\pi_4)^2(\pi_5)^2$ | | | | |

[a] Calculations were carried out at the B3LYP/6−31G* optimized geometry of the most stable rotamer, i.e. the *s,a*-rotamer (cf. Table 1). [b] For active space, see Section 2.3. [c] Percent contribution of the most important configurations to the CASSCF wave function (cf. MO plots in Figure 5). The $\sigma$-MO is doubly occupied except where indicated. [d] Oscillator strenghts. [e] Percent of the CASPT2 wave function described by the reference CASSCF wave function. [f] From the spectra in Figure 4. [g] Ground state.

**Table 3.** Excited States of **ECM**$^{\bullet+}$ [a] by CASSCF/CASPT2

| | CASSCF[b] | | CASPT2 | | | |
|---|---|---|---|---|---|---|
| state | $E_{rel}$/eV | composition[c] | $E_{rel}$/eV | $f$[d] | % ref[e] | exp $E_{rel}$/eV[f] |
| $1^2A''$[g] | (0) | 82% ... $(\pi_3)^2(\pi_4)^2(\pi_5)^1$ | (0) | | 69 | (0) |
| $2^2A''$ | 2.38 | 62% ... $(\pi_3)^2(\pi_4)^2(\pi_5)^0(\pi_6)^1$ | 2.07 | 0.015 | 69 | 2.06 |
| | | 8% ... $(\pi_3)^1(\pi_4)^2(\pi_5)^2$ | | | | |
| | | 6% ... $(\pi_3)^2(\pi_4)^1(\pi_5)^2$ | | | | |
| $3^2A''$ | 3.13 | 51% ... $(\pi_3)^1(\pi_4)^2(\pi_5)^2$ | 2.86 | 0.049 | 69 | $\approx$2.8 |
| | | 10% ... $(\pi_3)^2(\pi_4)^2(\pi_5)^0(\pi_6)^1$ | | | | |
| | | 9% ... $(\pi_3)^2(\pi_4)^1(\pi_5)^2$ | | | | |
| $4^2A''$ | 3.18 | 54% ... $(\pi_3)^2(\pi_4)^1(\pi_5)^2$ | 2.95 | 0.105 | 68 | $\approx$2.8 |
| | | 8% ... $(\pi_3)^2(\pi_4)^2(\pi_5)^0(\pi_6)^1$ | | | | |
| | | 6% ... $(\pi_3)^2(\pi_4)^2(\pi_5)^0(\pi_7)^1$ | | | | |
| $5^2A''$ | 4.31 | 37% ... $(\pi_3)^2(\pi_4)^2(\pi_5)^0(\pi_7)^1$ | 3.70 | 0.090 | 68 | >3.6 |
| | | 11% ... $(\pi_3)^1(\pi_4)^2(\pi_5)^2$ | | | | |
| | | 11% ... $(\pi_3)^1(\pi_4)^2(\pi_5)^1(\pi_6)^1$ | | | | |
| | | 5% ... $(\pi_3)^2(\pi_4)^1(\pi_5)^2$ | | | | |

[a] Calculations were carried out at the B3LYP/6−31G* optimized geometry of the rotamer where thje methyl group is *syn* to the ketene group. [b−g] See footnotes for Table 2.

on excited state calculations by the CASSCF/CASPT2 protocol. The results of these are displayed in Figure 4 which juxtaposes the EA features which we attribute to **VBA**$^{\bullet+}$ and **ECM**$^{\bullet+}$, respectively, to the CASPT2 predictions on an energy scale. Tables 2 and 3 list the corresponding numbers and assignments, including also those from the CASSCF calculations, whereas Figure 5 shows the MOs which are involved in the observed transitions. Firstly we note the very satisfactory quantitative agreement between experiment and theory[23] which gives us a degree of confidence that our assignments are correct.

In the *vinylbenzaldehyde cation* the first excited state is predicted to arise by ionization from the $\pi_4$ MO of **VBA** which corresponds essentially to a benzene HOMO (or by $\pi_4 \rightarrow \pi_5$ excitation in **VBA**$^{\bullet+}$). We could not observe any bands associated with **VBA**$^{\bullet+}$ in the NIR range, presumably because of the very small predicted oscillator strength of the corresponding EA transition, but the 1.16 eV excited state energy is in good agreement with $I_{v,2}-I_{a,1}$ in the photoelectron (PE) spectrum of **VBA**.[24] The EA band at 610 nm corresponds predominantly to a state arising by ionization from $\pi_3$ of **VBA** (or $\pi_3 \rightarrow \pi_5$ excitation in **VBA**$^{\bullet+}$), with a small admixture of the HOMO → LUMO excited configuration. It also shows up as the third band in the PE spectrum of **VBA**.[24]

According to CASPT2, the second, intense near-UV band of **VBA**$^{\bullet+}$ comprises *two* transitions of strongly mixed character. According to the calculations, the lower-lying state is to be associated with the 370-nm peak (in pefect quantitative agreement) whereas the higher-lying state must be buried in the UV tail of that band.

In the *quinoketene cation*, **ECM**$^{\bullet+}$, the analysis shows that the first excited state which gives rise to the sharp visible band is dominated by the HOMO → LUMO excited configuration, as is typical for the *o*-quinodimethane cation chromophore.[25] Again, the second EA band appears to comprise transitions to two excited states, again in excellent quantitative agreement with experiment. Both of these are dominated by Koopmans' configurations (ionization from $\pi_3$ and $\pi_4$, respectively) but carry substantial Non-Koopmans' contributions, i.e. excitations into virtual MOs. Finally, CASPT2 predicts another rather intense transition at 335 nm which is difficult to detect unambiguously because strong absorptions of the neutral precursor, **MBC**, begin to rise in this region. Nevertheless, the difference spectrum in Figure 4 indicates a band peaking at $\approx$325 nm whose position is in reasonable agreement with this prediction.

## 5. Conclusions

X-irradiation of the $C_9H_8O$ isomers, *o*-vinylbenzaldehyde (**VBA**) and 2-methylbenzocyclobuten-1-one (**MBC**), in solid argon in the presence of an electron scavenger leads to creation of a common *o*-quinoid ketene radical cation, **ECM**$^{\bullet+}$. Concurrently, the corresponding neutral **ECM** arises by re-neutralization of the cation which competes effectively with the added electron scavenger. B3LYP calculations predict that the predominant conformation of neutral **VBA** (80%) persists after

(23) It was impossible to achieve reasonable agreement with semiempirical methods. We attempted INDO/S calculations of **VBA**$^{\bullet+}$ and **ECM**$^{\bullet+}$, but as the SCF procedure invariably converged to a $\sigma$-state we could not evaluate the $\pi$-electronic structure by this method.

(24) Asmis, K.; Zhu, Z.; Bally, T. Unpublished. We thank Dr. Asmis (University of Fribourg) for recording this spectrum for us.

(25) Marcinek, A.; Michalak, J.; Rogowski, J.; Tang. W.; Bally, T.; Gebicki, J. *J. Chem. Soc., Perkin Trans. 2* **1992**, 1353.

ionization, which explains why the electronic absorption spectrum of **VBA**$^{\bullet+}$ could be very clearly detected after ionization of **VBA**. Conversely, the radical cation of **MBC** proved to be elusive, presumably because it is formed in a state which is dissociative with respect to ring-opening to **ECM**$^{\bullet+}$. The ketene stretching frequency of **ECM** is shifted to higher energies on ionization because the HOMO is C═O antibonding.

The EA spectra of **VBA**$^{\bullet+}$ and **ECM**$^{\bullet+}$ can be modeled very satisfactorily by CASSCF/CASPT2 calculations which give—apart from good quantitative agreement—a picture of the electronic structure in accord with qualitative expectations. This proves once again the validity and usefulness of this new method for modeling EA spectra of radical cations.[26]

**Acknowledgment.** This work has been funded through Grants No. 2028-047212.96 of the Swiss National Science Foundation and Grant No. 3.T09A.097.11 of the Polish State Committe for Scientific Research.

JA964243W

(26) See also: Fülscher, M. P.; Matzinger, S.; Bally, T. *Chem. Phys. Lett.* **1995**, *236*, 167. Truttmann, L.; Asmis, K. R.; Bally, T. *J. Phys. Chem.* **1995**, *99*, 17844.